SAE INTERNATIONAL

ARTICLE INFO
Article ID: 03-18-04-0028

doi:10.4271/03-18-04-0028

Ethanol Fuel as Enabler for High-Efficiency and Low-Soot Combustion in Dual-Fuel and Blend Modes

Giacomo Belgiorno,[1] Roberto Ianniello,[2] and Gabriele Di Blasio[2]

[1]Dumarey Automotive Italia S.p.A., Turin, Italy
[2]Consiglio Nazionale delle Ricerche, STEMS, Italy

Abstract

Global climate initiatives and government regulations are driving the demand for zero-carbon tailpipe emission vehicles. To ensure a sustainable transition, rapid action strategies are essential. In this context, renewable fuels can reduce lifecycle CO_2 emissions and enable low-soot and NOx emissions. This study examines the effects of renewable ethanol in dual-fuel (DF) and blend fueling modes in a compression ignition (CI) engine. The novelty of this research lies in comparing different combustion modes using the same engine test rig. The methodology was designed to evaluate the characteristics of various injection modes and identify the inherent features that define their application ranges. The investigation was conducted on a single-cylinder engine equipped with state-of-the-art combustion technology.

The results indicate that the maximum allowable ethanol concentration is 30% in blend mode, due to blend stability and regulatory standards, and 70% in DF mode, due to combustion stability and emission concerns. DF mode produces higher THC and CO emissions compared to blend or conventional diesel combustion (CDC) modes. However, ethanol consistently reduces smoke formation across all engine test conditions and fueling modes. At ultra-low-NOx levels (0.5 g/kWh), smoke emissions remain below 0.5 FSN. At the highest ethanol fraction in DF mode (70%), smoke emissions decrease to very low levels (−0.1 FSN), with improvements in thermal efficiency and CO_2 emissions. DF mode requires specific injection control strategies to mitigate THC and CO emissions. In blend mode, the highest ethanol fraction (30%) results in CO_2 and soot reductions, with CO and THC emissions comparable to CDC.

History

Received: 14 Jan 2025
Revised: 29 Apr 2025
Accepted: 19 Jun 2025
e-Available: 16 Jul 2025

Keywords

Renewable ethanol, Alcohol blends, Dual-fuel combustion, Ternary blends, Efficiency, Emissions

Citation

Belgiorno, G., Ianniello, R., and Di Blasio, G., "Ethanol Fuel as Enabler for High-Efficiency and Low-Soot Combustion in Dual-Fuel and Blend Modes," *SAE Int. J. Engines* 18(4):521-539, 2025, doi:10.4271/03-18-04-0028.

ISSN: 1946-3936
e-ISSN: 1946-3944

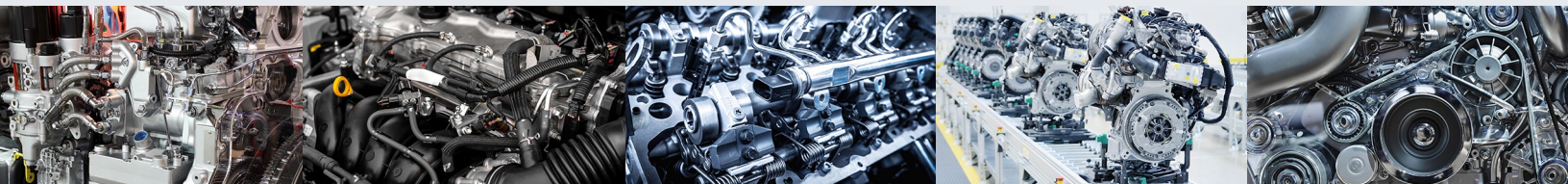

1. Introduction

In the short term, the transportation sector must meet stringent emissions standards aimed at reducing pollutant and greenhouse gas (GHG) emissions [1], with the goal of achieving net-zero emissions by 2050 [2]. Currently, the sector is responsible for about 16% of total GHG emissions, with on-road transportation applications accounting for approximately 12% [3]. Within this framework, renewable fuels may offer a viable solution, particularly for sectors where electrification is challenging, such as heavy-duty, aviation, and maritime transportation [4, 5].

To meet GHG reduction targets, high efficiency can be achieved by co-optimizing renewable fuels with innovative combustion engine technologies, further contributing to the decarbonization goal [6, 7]. Specifically, renewable alcohols can also be used with advanced combustion modes, dual-fuel (DF) or partially premixed combustion (PPC), enabling soot-less combustion and reducing life-cycle CO_2 [8, 9]. Alcohol fuels such as ethanol (EtOH) are particularly noteworthy as they can be produced from renewable energy sources by fermenting carbohydrates found in sugar cane, corn, rice, potatoes, and various fruits, using catalysts (enzymes) [10]. Ethanol is a low-carbon fuel since biomasses can almost entirely absorb the CO_2 produced from ethanol combustion ($0.96 kg_{CO_2}/kg_{fuel}$) [11]. It can partially or fully replace conventional fuels in both compression ignition (CI) and spark ignition (SI) engines. Indeed, it has a higher research octane number (RON) than gasoline but lower density and lower heating value (LHV) [12]. As a result, at the same thermal efficiency, approximately 11% more ethanol mass is required to achieve the target load of a gasoline-fueled engine. The higher heat of vaporization and lower boiling point induce a cooling effect, influencing the cold start phase. Additionally, the lower viscosity and lubricity of ethanol could impact the durability and functionality of engine components. CI engines can run on ethanol using various fuel injection strategies, either in blend mode or DF mode. Notably, DF mode requires modifications to the engine hardware and fuel injection system (FIS) [13].

Direct injection of neat ethanol in PPC mode on a heavy-duty CI engine has led to significant soot reduction at similar gaseous emissions and efficiencies [14, 15]. However, hardware modifications to the fuel injection system, such as the injector and high-pressure pump, are necessary to address ethanol's low lubricity. Blending ethanol with diesel in proper concentrations can meet fuel quality standards, though ethanol's hydrophilic nature limits its concentration to avoid phase separation. To extend this limit, anhydrous ethanol or blending agents are required [16]. Emulsifying agents can be added to produce a homogeneous mixture to suspend the small droplets or a cosolvent, which acts as an intermediate through molecular compatibility [17]. Biodiesel, acting as a surfactant, has been shown to effectively stabilize ethanol–diesel mixtures [18]. Ternary blends of ethanol, biodiesel, and diesel in various ratios have been tested in CI engines [16]. Using a 30% ethanol blend improved thermal efficiency by about 4% compared to conventional diesel combustion (CDC) and significantly reduced the soot–NOx trade-off [19]. A stationary application study confirmed that a 20% ethanol blend led to 7% and 32% reductions in NOx and soot emissions, respectively, compared to diesel mode, albeit with increased CO and HC emissions. At full load, thermal efficiency improved by 6%, while at partial load, ethanol application delayed the combustion phasing by about 2 crank angle degrees [20]. The mean particle size diameter decreased from approximately 200 nm (diesel) to 100 nm (ethanol blend), as also observed in [21]. Generally, ternary blends demonstrate superior performance in smoke and NOx emissions, albeit with a relative fuel consumption penalty. Their low-soot nature allows for higher exhaust gas recirculation (EGR) rates, achieving ultra-low-NOx emission levels. These blends have been shown to enhance the low-temperature combustion (LTC) operating range and increase maximum power output [22, 23]. Additives, including glyceric compounds, further improve emissions reduction in ethanol–diesel blends [24].

In DF applications in CI engines, the ethanol–diesel ratio can be tuned, maximizing the use of alcohol fuel across the engine operating map at the cost of increased complexity in the injection and control system design and operation. Various engine parameters, such as injection pattern, ethanol concentration, compression ratio, engine load, and speed, have been extensively studied in the literature [25, 26]. DF mode significantly affects the NOx–soot trade-off, while penalizing CO and THC emissions compared to CDC [27]. CO and THC emissions are primarily influenced by inlet temperature and ethanol concentration. Padala et al. [25] examined the effect of ethanol fraction in a CI engine under medium load, observing an efficiency increase of up to 10% compared to CDC, with a 60% ethanol fraction and advanced injection timing. Gawale and Naga Srinivasulu [28] investigated the DF strategy using a diesel–biodiesel blend as the directly injected fuel, with varying hydraulic nozzle flow rates. At full load, the highest flow rate achieved reductions of approximately 88% in smoke, 65% in NOx, and a slight 1.5% decrease in efficiency compared to CDC, while THC and CO emissions increased. Gargiulo et al. [29] reported similar outcomes, showing significant reductions in soot mass and particle number.

Overall, the literature indicates that while ethanol offers notable benefits in terms of engine performance and emissions reduction, its effective integration into compression ignition (CI) engines necessitates careful control of premixed or blending ratios, as well as close consideration of engine operating conditions to mitigate potential drawbacks. Both DF and blend strategies present viable pathways for reducing emissions and enhancing efficiency, yet the optimal approach depends

on specific engine configurations, performance targets, and regulatory constraints. DF systems typically offer greater flexibility in fuel utilization, whereas blend approaches provide simpler integration with existing engines and fuel infrastructure.

Despite the extensive research on ethanol-fueled CI and SI engines, comparative studies assessing the combustion and emission characteristics of ethanol-based DF and blend modes under identical engine platforms and boundary conditions remain scarce. The novelty of this work lies in the systematic evaluation and comparison of these combustion modes on a single-cylinder research engine equipped with advanced combustion technology. This controlled setup allows for direct assessment of ethanol's effects across different fueling strategies. The methodology is designed to characterize the behavior of various injection configurations, identifying the intrinsic features that define their operational ranges. The performance and emissions outcomes of each mode are benchmarked against CDC to elucidate their respective advantages and limitations in modern engine applications. Ultimately, this study aims to provide practical insights and technical guidance for the deployment of ethanol in existing internal combustion engines across diverse sectors such as transportation, off-road machinery, and power generation.

2. Experimental Setup and Test Procedures

This section summarizes the main characteristics of the experimental setup and the fuels tested during the test campaign. It then explains the test methodology and procedure adopted for the proposed research.

The experimental activities were performed using a 0.5 dm^3 CI single-cylinder engine (SCE). This setup is highly flexible, allowing for variations in key engine control parameters such as boost and exhaust pressures, fuel injection settings, and EGR rate. The engine setup is illustrated in Figure 1. A port fuel injector (PFI) is mounted on the intake manifold near the intake valves and connected to a specific pressure regulator for ethanol fuel. In the DF configuration, a constant start of injection at 360 crank angle degrees before the firing top-dead center (bTDC) was used for the ethanol injection. A state-of-the-art direct fuel injection system with a seven-hole solenoid injector was used. The combustion chamber featured a conventional diesel omega-piston bowl shape. The main features of the SCE are shown in Table 1.

The boost, exhaust pressures, and EGR levels were managed through pneumatic valves controlled by NI CRIO

FIGURE 1 Schematic of the research engine setup and emission measurement system.

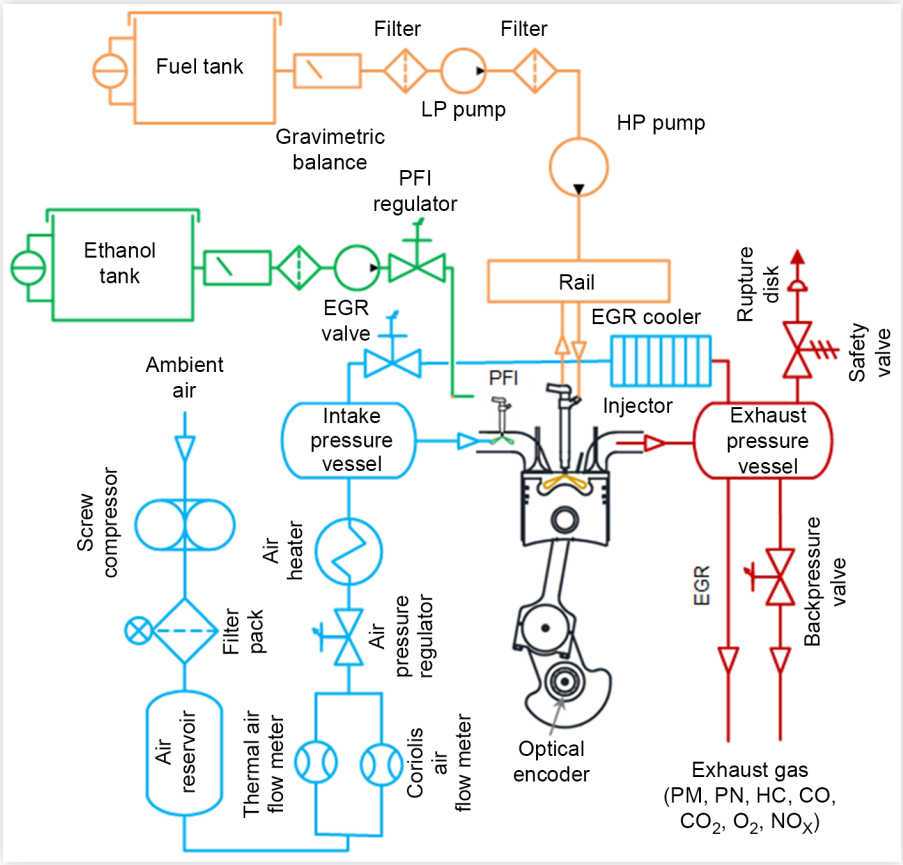

TABLE 1 SCE characteristics.

Engine type	CI-SCE, 4 valves		
Displacement volume	0.5 dm^3		
Bore × stroke	82 mm × 90.4 mm		
Piston geometry	ω-bowl		
Compression ratio	16.0:1		
Diesel fuel injection system	Common rail with solenoid injector (up to 2000 bar)		
Injector number of holes	7		
Port fuel injection system	Multi-hole solenoid injector		
In-cylinder swirl ratio	2.5		
Valve timing		Inlet	Exhaust
	Opening time	350°bTDC	123°bTDC
	Closing time	−137°bTDC	−345°bTDC

FPGA hardware and NI LabVIEW software. This setup provided the flexibility to replicate the engine-like conditions of a multi-cylinder engine. For the fuel injection systems, both PFI and DI, the software was used to monitor and control the start of injection (SOI), injection pressure, energizing time, and number of pulses.

The lubricating oil, coolant, and intake air engine conditions were monitored and controlled through external conditioning systems to maintain constant boundary conditions. A Kistler 6125C piezoelectric pressure sensor was employed to detect the in-cylinder pressure, mounted in the glow plug seat, and connected to a Kistler amplifier. The in-cylinder pressure traces were recorded with a resolution of 0.1 crank angle degrees and averaged over 300 cycles. The apparent heat release (HR) and heat release rate (HRR) were calculated based on the in-cylinder pressure, actual volume as a function of crank angle, and specific heat ratio using real-time AVL software. Based on the post-processing of the signals, correlated combustion parameters such as IMEP (indicated mean effective pressure), CA10, CA50, and CA90 (angle positions where 10%, 50%, and 90% of the total HR, respectively), and pumping losses were calculated [30]. The ignition delay (ID), expressed in crank angle degrees, is calculated as the difference between the CA10 and the SOI of direct injection. Similarly, CA10-90 indicates the combustion time necessary to complete the combustion process, calculated as the difference between CA10 and CA90.

The AVL 733 gravimetric balance was used to measure the fuel consumption. The pollutant emissions were measured using a HORIBA MEXA 7100H emissions test bench, which recorded THC, CO_2, O_2, CO, and NOx at the exhaust and O_2 and CO_2 at the intake. Emissions were measured under steady-state conditions and averaged over at least 60 s. The EGR rate was evaluated as the ratio between the intake and exhaust CO_2. The smoke number was detected using the smoke meter AVL 415S. The measurement of the particles' distribution at the exhaust would have been very interesting but not possible at the time the authors conducted the experiments.

TABLE 2 Fuel properties.

Fuel properties	Diesel	Biodiesel	Ethanol
RON [—]	—	—	108
CN [—]	53	51	—
H/C ratio [—]	1.8	1.79	3.0
O/C ratio [—]	0	0.11	0.5
Stoichiometric air/fuel ratio [—]	14.5	13.8	9.0
Lower heating value [MJ/kg]	43.2	37.0	26.9
Viscosity [mm/s^2]	3.91	>6	1.36
Boiling point [°C]	188–343	182–338	78
Enthalpy of vaporization [kJ/kg]	−300	−350	920

Table 2 shows the relevant chemical and physical properties of the fuels used, collected and averaged where possible [16, 31–34]. Hereafter, some brief explanation about the reasoning behind the ethanol percentage used in both blend and DF combustion modes. Ethanol is characterized by a low boiling point, high latent heat of vaporization, and lower viscosity and density. Thus, volumetric efficiency may increase due to the in-cylinder charge cooling effect, at the expense of issues in cold start conditions [13, 35]. Ethanol's shorter molecular chain, oxygen content, and higher H/C ratio in comparison to diesel ratio may speed up the combustion process and reduce emissions [36]. Its polar nature can cause in-phase separation [37]. Literature studies demonstrated that EtOH concentration in diesel should not exceed 25% to avoid modifications to the diesel injection hardware [35]. The presence of biodiesel in the blend acts as a solubilizer, allowing for an increased ethanol content in diesel [15, 30, 31]. Temperature affects the stability of the blend, with phase separation occurring below 10°C. In such conditions, isopropanol can act as a stabilizer [17].

The European EN 288 standard and the 2009/30/EC directive prescribe a maximum limit of 10% v/v of ethanol in gasoline to ensure compatibility with most engines on the market [38]. On the other hand, ethanol in diesel impacts lubricity and kinematic viscosity, potentially causing durability issues in injection system components [39]. To this aim, the authors have collected data from the technical literature [40–45] and normalized it to provide essential information, through a single graph, to current EN 590 standards. Indeed, Figure 2 shows the kinematic viscosity and wear scar diameter (WSD) as a function of the ethanol concentration.

It can be stated that the reduction in viscosity is evident with the increase in ethanol. However, blends with about 30% ethanol are still compliant in terms of viscosity. For higher ethanol concentrations, the DF strategy is recommended. Based on this evidence, the ethanol

FIGURE 2 Kinematic viscosity and WSD dependencies of the ethanol fraction in diesel–biodiesel blends at 40°C.

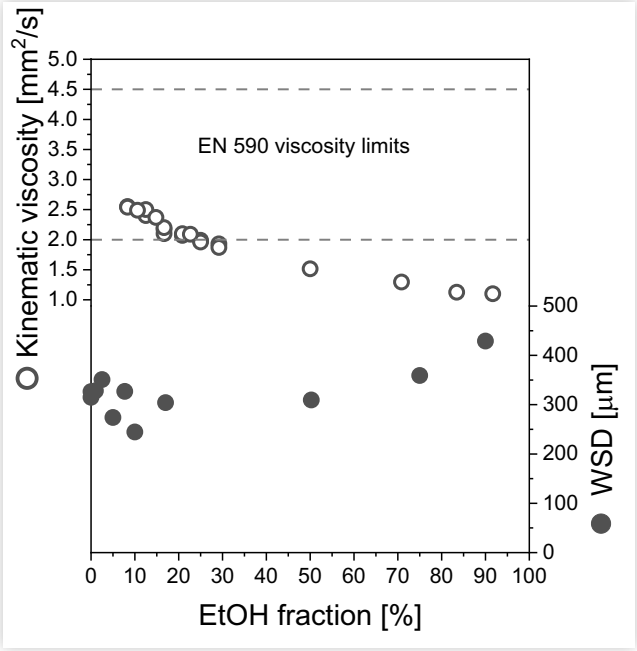

concentration in the ternary blends made of diesel, ethanol, and biodiesel, and used within this study, has been limited to 30%. Complementary, in DF mode, the ethanol concentration has been varied from 30% to 70%.

The lubricity of diesel–ethanol blends decreases with ethanol. According to EN 590:1999, the lubricity test (ISO 12156-1), the corrected WSD should not exceed 450 µm. The studies from which the data are collected have demonstrated that the WSD value of diesel–ethanol blends with ethanol concentrations of 90% v/v exceeds this limit, reaching 460 µm. On the other hand, for blends with 30% v/v ethanol, the values remain well below this limit [43].

It is important to highlight that ethanol-based blends may promote the oxidation processes attributed to ionic impurities, water content, and the polarity of the ethanol molecule [32]. The corrosion rate increases in the presence of copper, aluminum, and stainless steel [46]. A weight reduction of all metal parts immersed in different blend samples was observed, ranging between 0.1 and 0.2 mg over a limited observation period [45]. Aluminum has demonstrated a higher resilience to corrosion [47].

Moreover, the ethanol–biodiesel–diesel blend stability tests for ratios of 68:17:15 and 58:14:30 were conducted again for this test campaign. As for previous tests, soybean methyl ester (SME) was used as a solubilizer [16]. No phase separation was detected during the observation period of the test campaign. It would be interesting to extend much more this period. In DF mode, three levels of ethanol fraction were injected via PFI (–30%, –50%, –70% v/v), allowing for greater flexibility in the fraction control.

The test campaign was designed to assess the effect of ethanol in achieving ultra-low-NOx emission targets or defining the operating domain for blend and DF modes. To this aim, ethanol concentration and EGR rate sensitivities were studied for both DF and blend fueling modes. The results were compared to the CDC mode. Medium engine speeds (1500, 2000 rpm) and loads (7, 10 bar of IMEP) were investigated. CDC engine calibration was used as a reference. For the analysis, one parameter at a time was varied, such as combustion phasing (CA50) and injection pressure. The boost and intake manifold temperature values were derived from CDC settings and kept constant for both fueling modes. The approach was to maintain high efficiency in all combustion modes tested. Fuel injection pressure and CA50 were defined for CDC, as they represent the optimal balance between efficiency and combustion noise. These parameters were used as a reference for both DF and blend strategies.

Regarding the blend mode, the injection pattern of the CDC was adopted, and the SOI was tuned to reach the same CA50 target. This approach was employed to assess the reliability of the blend fueling mode, given that the system did not require modifications to the injection system. In contrast, the DF mode has necessitated a recalibration of the diesel injection to better distribute the high-reactivity fuel into the combustion chamber to better control and stabilize the combustion. A combustion noise limit of 95 dBA and a THC limit of 2500 ppm (–9.8 g/kWh) were established to preserve combustion efficiency. It was observed that single-pulse DI injection resulted in combustion noise values exceeding the desired range, although it exhibited slightly higher efficiency values than the multi-injection pattern.

Regarding the DF mode, the tests were carried out using a multi-injection strategy for direct injection, which provided the optimal compromise in terms of efficiency, combustion noise, and stability [48]. In general, the tests were performed following the same approach as for the blend mode (i.e., SOI tuning to reach the CA50 target of CDC). The main operating settings used for the experimental campaign are shown in Table 3.

An analysis of both injection modes (DF and blend) in terms of the combustion process and emissions was performed under steady-state conditions at two operating points. Specifically, the method applied is oriented toward the following results:

1. Assess the impact of the EtOH fraction on global engine performance within the operating domain of convenience for both combustion modes. The ranges investigated are complementary and vary from 0% to 30% in blend mode and 30% to 70% in DF mode.
2. Evaluate the EGR rate sensitivity at the maximum EtOH concentration for each fueling mode (30% in blend and 70% in DF) by increasing the EGR rate (up to 50%) to achieve ultra-low-NOx values.

TABLE 3 Test matrix and engine settings.

Combustion mode	CDC	EtOH—DF	EtOH—blend
Engine speed [rpm]	1500 | 2000		
IMEP [bar]	7.0 | 10.0		
Boost pressure [kPa]	115 | 120		
EGR rate [%]	0–50		
T intake manifold [°C]	60 | 65		
Injection pressure [MPa]	76.5 | 91.5		
CA50 [aTDC]	−8 to −10		
EtOH fraction [%]	0	30–50–70 | 70	15–30
Direct injection pattern	Pilot/main	Pilot1/pilot2/main	Pilot/main

3. Compare DF and blend combustion modes, at their maximum EtOH fraction, to the CDC in the ultra-low-NOx emissions area (0.5–1.0 g/kWh).

The mass-based ethanol premixed ratio (r_p) is defined according to Equation 1:

$$r_p = \frac{m_{ethanol}}{m_{ethanol} + m_{diesel}} \times 100\left[\%\right] \quad (1)$$

where the m_{diesel} and $m_{ethanol}$ mean the mass flow rate of diesel direct injection and ethanol fuel (PFI), respectively, while the LHV_{diesel} and $LHV_{ethanol}$ are the LHV for each fuel. The average LHV is calculated as in Equation 2:

$$LHV_{mix} = \frac{m_{ethanol}}{m_{tot}} \times LHV_{ethanol} + \left(1 - \frac{m_{ethanol}}{m_{tot}}\right) \times LHV_{diesel} \quad (2)$$

The generic X engine-out emission mass flow rate (m_X) were referred to the indicated specific power (P_{ind}) to calculate the indicated specific emissions (isX) by the following equation:

$$isX = \frac{m_X}{P_{ind}}\left[\frac{\text{g}}{\text{kWh}}\right]$$

The energy balance analysis assesses the energy distribution and process losses, and the main factors affecting the gross indicated efficiency (η_{gross}) and fuel consumption. Figure 3 reports the energy balance terms and equations [30]. The various terms include the fuel energy $\left(\dot{Q}_{fuel}\right)$ into the gross indicated work $\left(\dot{W}_{gross}\right)$ and energy losses such as incomplete combustion $(1 - \eta_{comb})$, in-cylinder heat transfer (heat transfer loss), and exhaust energy $\left(\dot{m}_{Exh} h_{Exh}\right)$, where h_{Exh} is the enthalpy content of the exhaust mass flow.

The combustion loss represents the fraction of unburned fuel energy from incomplete combustion. Heat transfer (HT) losses are defined as convection heat (oil and water coolant) and radiative heat losses. The exhaust losses are the enthalpy content available at the engine exhaust.

Uncertainty analysis is fundamental to identifying potential sources of error and assessing their impact on the overall outcomes. To this aim, the experiments were performed three times and averaged. The uncertainty and the accuracy of instruments are listed in Table 4. The combined uncertainty (u_{comb}) was computed using the root mean square method (error propagation method) $u_{comb} = \sqrt{\sum_i^n \left(u_i\right)^2}$ [49].

3. Results and Discussion

This section discusses the experimental results for both DF and blend modes, focusing mainly on the combustion process, engine-out emissions, and efficiencies. The results are then compared with the CDC data. First, the analysis addresses the sensitivity of the ethanol premixed ratio on

FIGURE 3 Energy balance calculation.

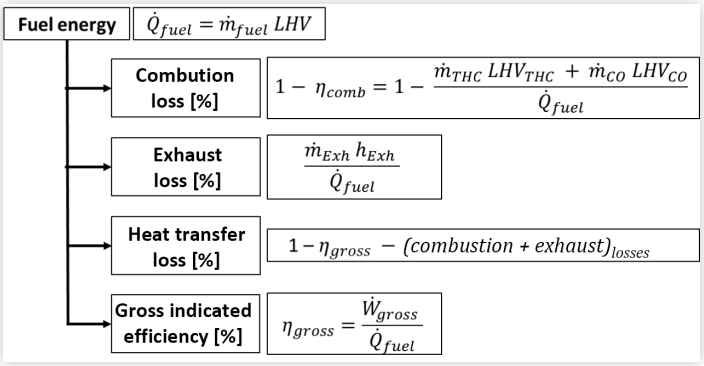

TABLE 4 Uncertainties of instruments used in experimentation.

Measurement	Accuracy	Uncertainty (%)
Load	±1 N	±0.2
In-cylinder pressure sensor	±0.4% FS	±0.4
Crank angle—encoder	±0.02°	±0.2
Fuel mass flow rate	±0.1 kg/h	±0.2
Air mass flow rate	±1 kg/h	±0.5
k-type thermocouple	±2.5°C	±1.0
Gas species [O_2, CO_2, CO, THC, NOx]	±2.5% FS	±0.6
Smoke	±0.025 FSN	±0.5

the main engine outputs to determine the effect of alcohol fuel. Next, the sensitivity of the EGR rate on NOx, soot trade-offs, gross indicated efficiency, and related combustion processes are discussed for both strategies. Finally, a comparison between the ethanol combustion modes investigated and CDC is presented at low-NOx emission levels. Additionally, the results and trends observed are compared with findings from the literature review. This section summarizes the main opportunities and challenges of ethanol combustion applications compared to the CDC baseline, aiming to provide guidelines for practical ethanol applications in internal combustion engines.

3.1. Ethanol Premixed Ratio

This section presents the results of the impact of different ethanol premixed ratios (r_p) in DF and blend modes on the combustion process, emissions, and gross indicated efficiency. The results are also compared to the CDC. The motivation for this analysis is, first, to discriminate the effect of the ethanol ratio on the global performance without the combined influence of other parameters, and second, to emulate the application of ethanol on existing engines without substantial modifications and not using EGR. This is the case, for example, with older stationary or off-road engine applications.

The high vaporization tendency and low chemical reactivity of ethanol enhance mixture homogeneity in both blend and DF cases. However, the polar nature of ethanol limits the maximum concentration in diesel blends. In this study, biodiesel was used as a solubilizer to ensure a stable blend with ethanol concentrations of up to 30% v/v. For higher concentrations (r_p > 30%), the application of DF technology is necessary. As known from the literature, one of the main issues with DF mode is the increase in unburnt emissions. Therefore, during the test campaign, THC was limited to 2500 ppm (–9.8 g/kWh) to preserve combustion efficiency. This limit was never reached in blend mode, while in DF mode, it was reached for r_p of 70% (Figure 4), the maximum ethanol

FIGURE 4 Gross indicated efficiency and pollutant emissions for the different r_p at 1500 rpm—7 bar IMEP.

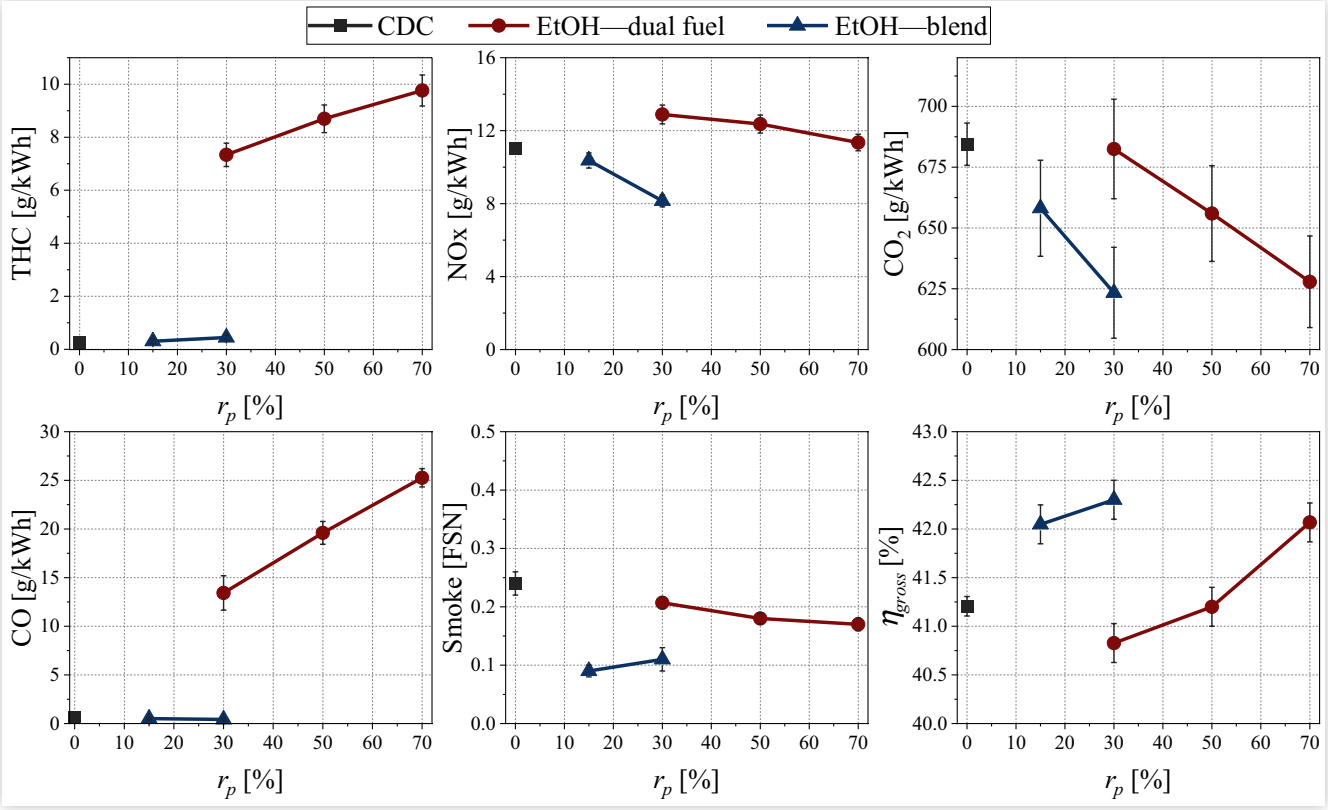

fraction used in DF mode within this study. Gaseous emissions (THC, CO, NOx), smoke, CO_2, and η_{gross} as a function of the r_p are shown in Figure 4 for EtOH and CDC fueling modes. The results refer to the operating point at 1500 rpm and 7 bar of IMEP at constant boundaries (pumping work, direct fuel injection pressure, and CA50). EGR was not employed at this stage to discriminate the r_p effect only. The SOI of the direct injection was properly varied to maintain the desired value of CA50 (in the range of 8–10°aTDC). In contrast, the dwell times among the injection pulses were not varied.

DF mode leads to a significant THC increase mainly related to the fuel mixture trapped in squish and crevice volumes during the compression stroke before the ignition phase. The higher crevice volumes and compression ratio of CI engines emphasize the THC increase [49]. This result is confirmed by 3D CFD studies showing that in DF mode, unburned methane emissions were mainly confined in the crevice volumes [50]. CO emission increase relates to the premixed ratio and lower in-cylinder temperatures of the DF modes. Cooling effects and higher mixture homogeneity are the main causes. The increase in r_p, in the range of 30%–70%, leads to a quasi-linear rise in THC and CO emissions (Figure 4). This trend is particularly evident at low loads. Indeed, as observed by other studies [51], at r_p = 17%, an increase in THC emissions (1.5 to 4.5 g/kWh) was observed when the engine load was reduced from 10 to 2 bar IMEP.

The blend combustion mode resulted in slightly higher CO and THC emissions than CDC, but lower than the DF mode. This is due to the lower concentrations of ethanol and the reduced residence time before the start of combustion compared to DF mode. Instead, comparing the results to the CDC, the higher unburnt hydrocarbons are justified by the cooling effect of ethanol, the lower reactivity of the mixture, the reduced effectiveness of the pilot combustion, and the lower combustion temperatures (confirmed by the NOx trend) [52, 53].

The overall NOx values detected were relatively high (>8 g/kWh) without EGR (Figure 4). Looking at the maximum r_p, in blend mode, a fraction of 30% EtOH reduces NOx emissions by −25%, while in DF mode, a fraction of 70% EtOH reduces NOx emissions by −16% compared to the results at the minimum r_p level. The lower NOx emissions are mainly attributable to the local ethanol cooling effect. The cavitation phenomenon resulting from the increase in ethanol fraction promotes a more vigorous flow near the nozzle, which reduces air–fuel mixing and the temperatures inhibiting the NOx formation [54].

For both combustion modes, the smoke level tends to reduce below the CDC values. EtOH in the blend reduces the smoke to 55%, while DF mode exhibits comparable levels compared to the CDC. In general, the lower soot emission of ethanol combustion is mainly related to the higher H/C ratio (shorter carbon chain), which facilitates the reduction of precursor molecules primarily responsible for pyrolysis. When alcohol fuels are injected in PFI mode, the local equivalence ratio decreases in the diesel spray area, causing an increase in the ID and resulting in more premixed combustion and less smoke formation. Nevertheless, in DF mode, as the mass fraction of ethanol rises, particularly under high load conditions, the available oxygen can be markedly diminished, potentially increasing smoke emissions [53]. This trend is illustrated in Figure 4, where the smoke level is comparable to the CDC and tends to increase slightly with the highest premixed ratio.

The gross indicated efficiency (η_{gross}) is plotted as a function of the r_p. CDC has an η_{gross} of about 41.2%. For 50% of r_p, DF has a comparable efficiency. Rising the r_p to 70%, η_{gross} reaches values up to −42.0%, higher than the CDC baseline despite the higher THC and CO emissions. This relates to the increased premixed combustion stage and shorter combustion duration (CA10-90) by about 8°, improving the cycle conversion efficiency. EtOH blend of 30% exhibits the highest efficiency (−42.3%). These results can be attributed to the higher cooling effect and the reduced combustion duration (CA10-90). These factors lead to lower heat losses and higher thermodynamic efficiency. Figure 5 depicts the apparent HRR, direct fuel injection profiles, and combustion durations (CA10-50 and CA50-90) varying the r_p. The SOI was varied to maintain constant the CA50 in the 8–10°aTDC range. The test procedure section described a multi-injection pattern implemented in DF mode, while a double-pulse strategy was used in CDC and EtOH blend cases.

In DF mode, by increasing the ethanol fraction from 30% to 70%, the peak of the HRR advances 5°aTDC, with a pronounced premixed phase and faster combustion, as demonstrated by the CA10-50 and CA50-90 indicators, respectively. The combustion duration reduces by about 3°, and the η_{gross} increases by −1%. Despite the slightly advanced premixed stage and reduced CA10-90, the smoke emissions remain almost constant (−0.2 FSN) regardless of r_p. In this case, the theoretical benefit of ethanol is counteracted by the ethanol fuel enrichment around the diesel spray.

The ethanol–diesel blend combustion has a longer ID because of the lower fuel reactivity than diesel fuel. This impacts the effectiveness of the pilot heat release, as observed by the HRR traces in Figure 5. However, since the CA50 is adjusted by advancing the injection pattern, the premixed phase is almost like the CDC for both r_p cases (15% and 30%).

The DF and blend mode employing the maximum r_p, 70% and 30%, respectively, reduce the CO_2 up to −7.5% compared to CDC and are related to the combined effect of higher gross indicated efficiency and lower carbon fuel content. Based on these results, the highest ethanol ratios for both combustion modes have been chosen for further analyses in Sections 3.2 and 3.3.

FIGURE 5 HRR, injection profiles, and combustion durations for both modes and different ethanol fractions at 1500 rpm and 7 bar IMEP.

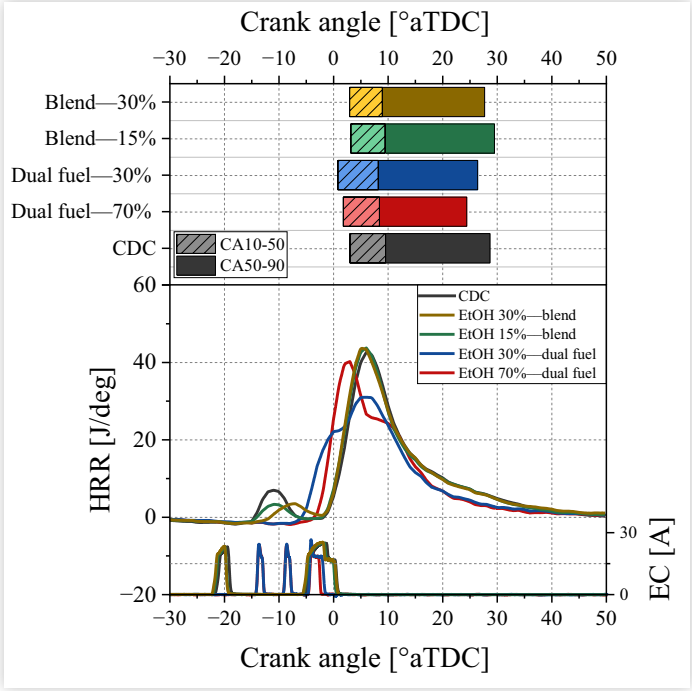

3.2. Ethanol as Low-NOx–Soot Enabler

The effectiveness of ethanol as a soot suppressor in the ultra-low-NOx emission combustion control region is investigated in this section. The EGR rate is one of the main factors used to control NOx emissions. The EGR rate sensitivity was evaluated at 1500 rpm and 7 bar of IMEP. The highest ethanol fractions were investigated for blend and DF combustion modes, which are 30% and 70%, respectively. The same boundary conditions were used, and the SOI was tuned to maintain the CA50 constant.

In CDC mode, NOx values below 0.5 g/kWh are for EGR rates higher than 40%, but at the expense of very high smoke levels (>3.2 FSN). The exponential growth of smoke results from reduced oxygen availability and an amplified diffusion stage [55]. Conversely, since ethanol fuel is a relatively simple molecule containing two carbon atoms connected to the OH_- group and has a short carbon chain, the structure generally yields a lower tendency to form polycyclic aromatic hydrocarbon (PAH) precursors of soot formation [56, 57]. Indeed, it is demonstrated that EtOH combustion resulted in low levels of particle number and soot [58]. Soot reduction is mainly linked to the higher premixed combustion phase and lower carbon content of ethanol than diesel fuel. This leads to decreased precursor molecules, which are primarily responsible for pyrolysis and, subsequently, particulate matter formation [56]. Additionally, biodiesel used as an emulsifier for the blend further reduces the carbon intensity, contributing to the soot reduction. As shown in Figure 6, with 30% ethanol in the blend, smoke does not exceed −0.5 FSN even for high EGR rates (−40%) and achieves ultra-low-NOx values (−0.5 g/kWh). When operating in DF mode at higher ethanol concentrations (r_p = 70%), the soot emissions remain consistently low (<0.3 FSN) for all the investigated EGR rate levels, with the advantage of keeping under control the smoke emission values independently of the NOx level. Figure 6 shows that EGR exerts a relatively modest influence on soot, with the high ethanol fraction contributing significantly to its reduction. In blend mode, soot increases slightly as EGR rises since the dilution effect increases the diffusive combustion stage compared to the DF. Thus, in both cases, ethanol has the potential to significantly optimize the NOx–smoke trade-off and achieve values below 0.5 FSN and 0.5 g/kWh for smoke and NOx, respectively.

For EtOH blends, the increase of EGR leads to higher HRR peaks (−20 J/deg., see violet trace in Figure 7). The high EGR rate reduces the in-cylinder temperature without a detrimental effect on the combustion duration. Consequently, the in-cylinder heat flux through the cylinder walls (or HT losses decrease) raises the η_{gross} by 4% compared to the case without EGR (Figure 8). Comparable differences are also evident when comparing

FIGURE 6 NOx–smoke trade-offs for DF, blend, and CDC modes at 1500 rpm—7 bar IMEP.

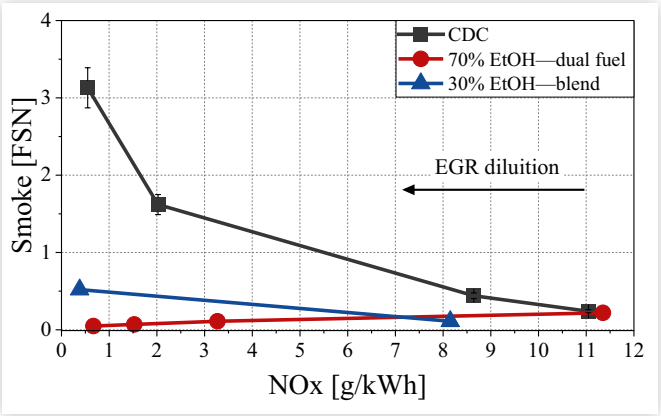

FIGURE 7 HRR, injection profile, and CA10-90 for different combustion modes and EGR levels at 1500 rpm—7 bar IMEP.

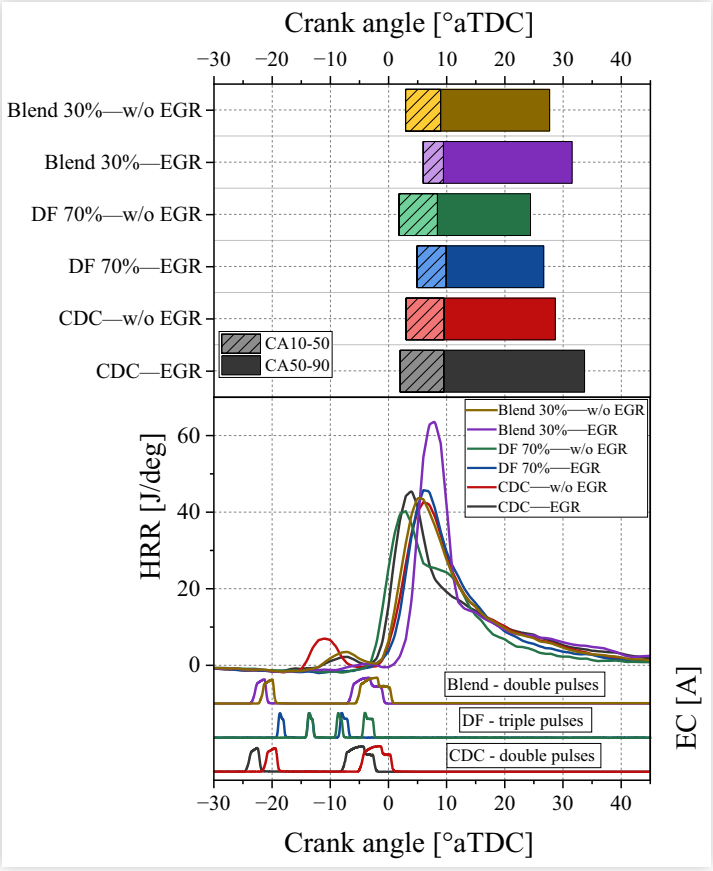

FIGURE 8 NOx – η_{gross} trade-off for CDC, DF, and blend combustion modes at 1500 rpm—7 bar IMEP.

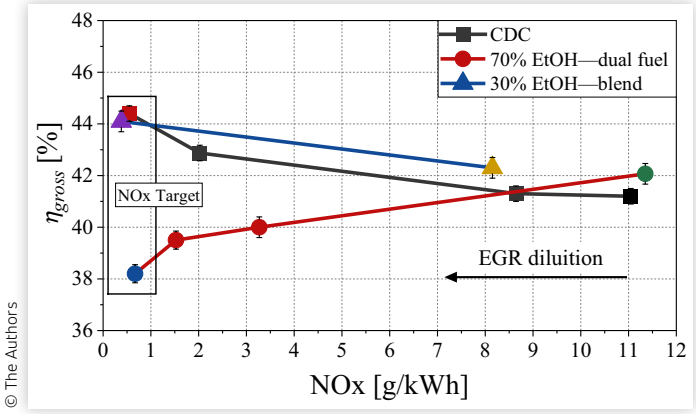

the EtOH blend to the CDC mode using EGR. A reduction of approximately 6° in combustion duration and an increase of –18 J/deg. on the HRR peak are observed at the same NOx (–0.5 g/kWh). This leads to a rise of 2% in η_{gross} compared to the CDC. A higher EGR rate in DF mode results in a longer ID (–3°) compared to the no EGR case. Consequently, there is a slight delay in CA50 and an increase in the peak of HRR (–5 J/deg.), which is lower than the sensitivity observed with the blend combustion.

Figure 8 shows the NOx – η_{gross} correlation for the investigated combustion modes. For CDC mode, the η_{gross} increases by –3% when moving from the no EGR to the maximum EGR rate (–40%). The higher EGR rate reduces diesel reactivity and the low-temperature HR in the initial stage of the combustion process, resulting in a longer ID in comparison to the no EGR case. Consequently, the efficiency improvement is associated with the higher premixed combustion phase and lower HR before the TDC (Figure 7).

For low NOx (–0.5 g/kWh), DF combustion has a lower η_{gross} of –6% units than CDC (Figure 8). It is worth mentioning that the diesel combustion chamber tested significantly influences DF rather than the blend mode. This is evident mainly for high EGR dilution ratios combined with higher EtOH fractions, which emphasize the quenching phenomenon, particularly in the squish and crevice volumes [59, 60], producing high THC and CO emissions. This outcome results from the combustion architecture that exploits the direct-injected fuel spray.

In conclusion, using EtOH-based fuels in combination with EGR strategies offers significant advantages in reducing emissions and improving thermodynamic efficiency. The results show that the EtOH blend combustion improves the η_{gross} by –2% and –8% compared to CDC and DF, respectively, at ultra-low-NOx levels (–0.5 g/kWh). For the explored operating points, the EGR strategy is more beneficial for the blend mode, as it permits very low smoke values and marginal efficiency gains for low-NOx values to optimize engine performance. The DF mode is very effective on the NOx–smoke trade-off at the expense of higher unburnt and lower efficiency.

3.3. Comparison of Different Ethanol Combustion Applications

This section focuses on the comparative analysis of the combustion process (Figure 9), combustion parameters, emissions (Figure 10), and efficiencies (Figure 11) of both DF and blend combustion modes at the maximum ethanol ratios, which are 70% and 30%, respectively. Two operating points, 1500 rpm and 7 bar IMEP, and 2000 rpm and 10 bar IMEP, were selected at almost constant CA50 (in the range of 8–10°aTDC) and NOx (<1.0 g/kWh). The results are compared to the CDC. The NOx values were tuned to very low levels through EGR, at –0.5 and –1.0 g/kWh for 7 and 10 bar IMEP, respectively. The test points represent frequently operated part-load conditions of light-duty multi-cylinder engine applications. This analysis aims to highlight the benefits and drawbacks of these combustion modes and to provide valuable evidence as to which mode offers the most remarkable advantages toward cleaner and more efficient engine technologies without significant modifications to the CI application. To this aim, a Pugh matrix of ethanol for different combustion modes in comparison with CDC is discussed in this section.

HRR traces with corresponding injector signals and combustion durations for DF, blend, and CDC modes are shown in Figure 9. The use of ethanol has a considerable influence on the combustion process. Its low reactivity and volatility lead to a greater ID. This behavior is a function of the ethanol percentage and the operating point. As shown in Figure 10, at 1500 rpm, a delay of about 5° is observed for both combustion modes. This gap is reduced at higher loads as the thermodynamic conditions in the combustion chamber become more significant than the chemical-physical properties. A longer

FIGURE 9 HRR, injection profiles, and combustion duration for EtOH combustion modes and CDC at two operating engine conditions.

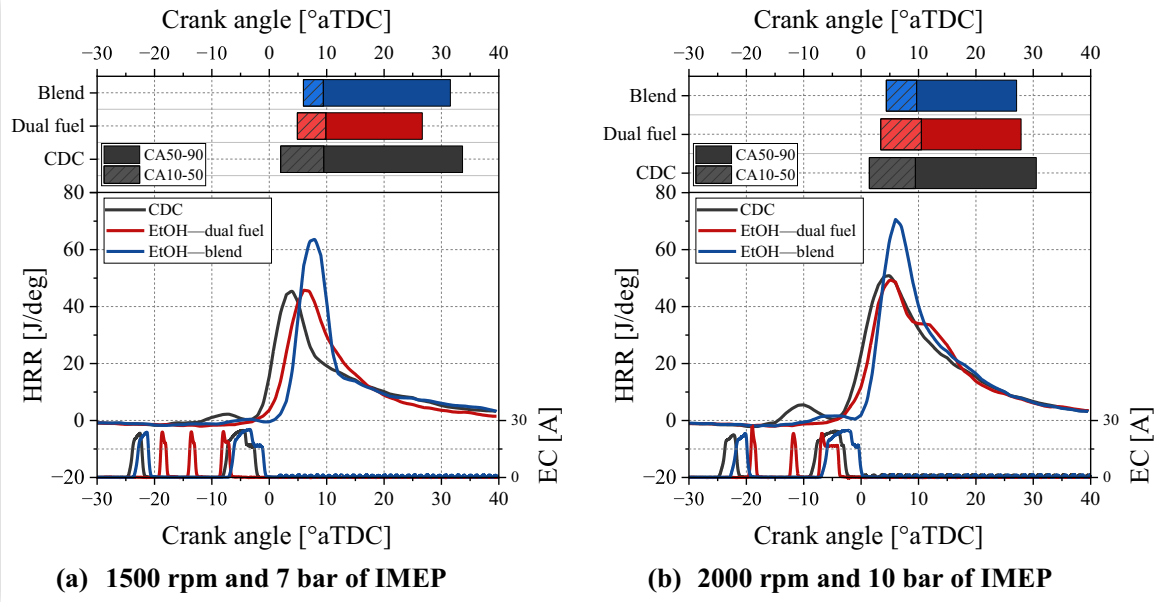

FIGURE 10 Engine global performances for EtOH and CDC combustion modes at two operating engine conditions, 1500 rpm—7 bar IMEP (left) and 2000 rpm—10 bar IMEP (right).

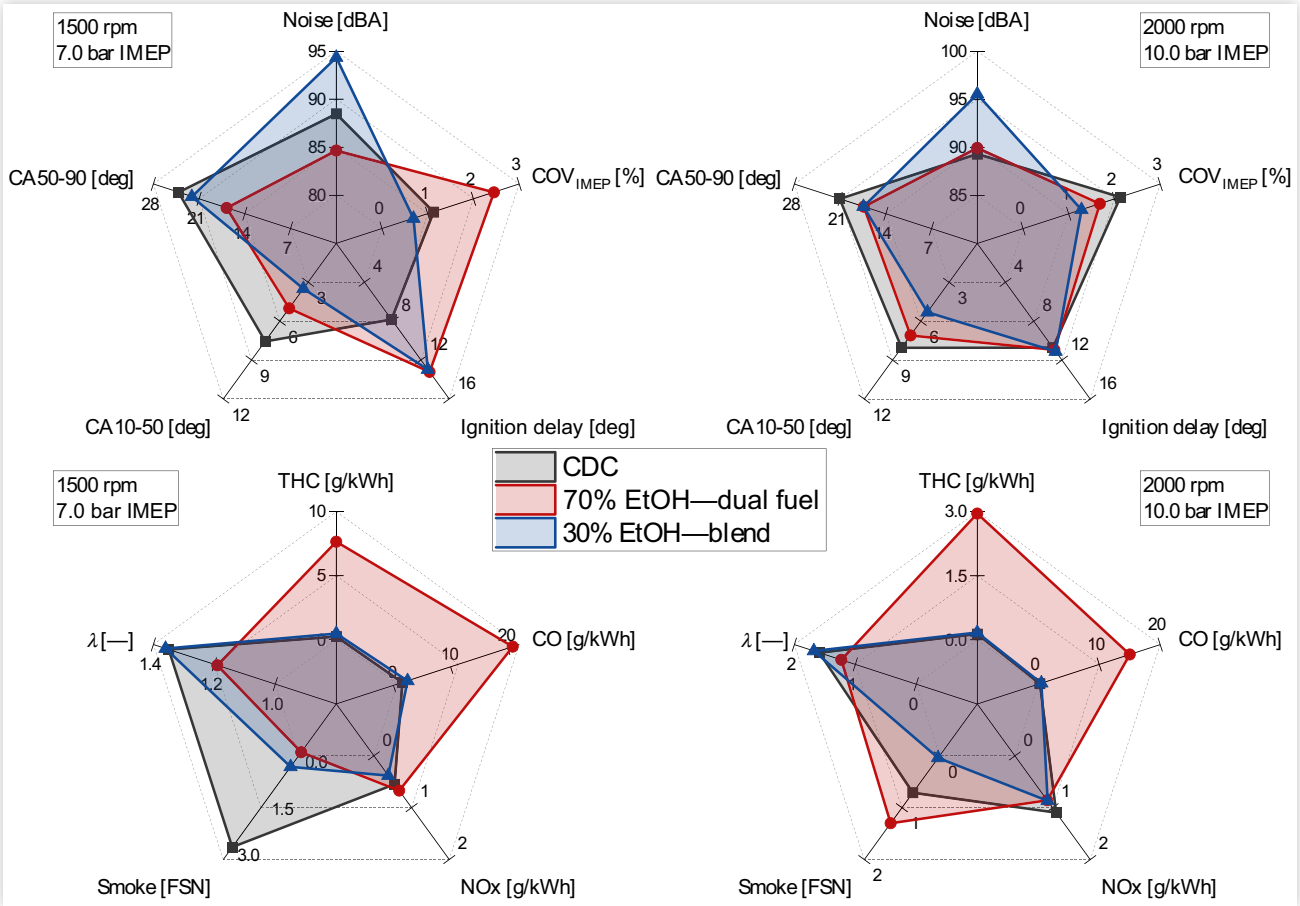

FIGURE 11 Energy distributions for EtOH and CDC combustion modes at two operating engine conditions, 1500 rpm—7 bar IMEP (left) and 2000 rpm—10 bar IMEP (right).

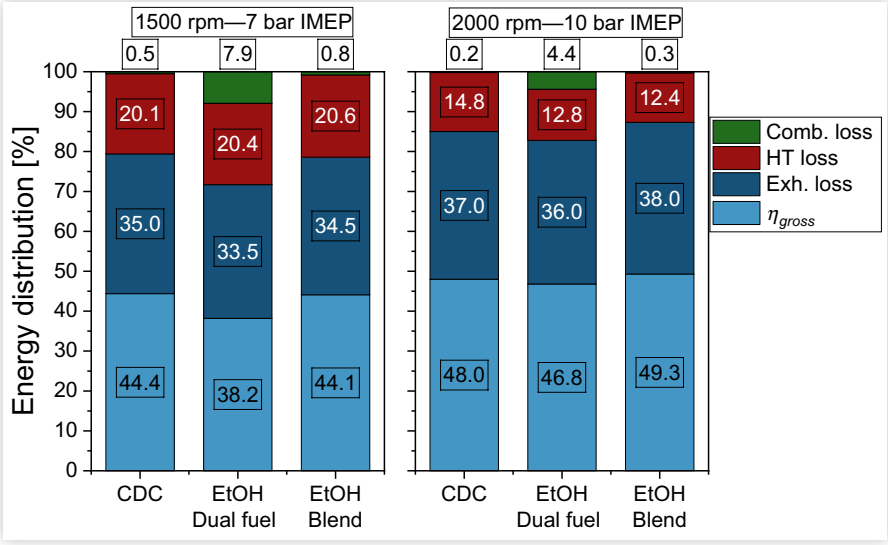

ID and the higher heat of vaporization of ethanol, which cools down the mixture, resulted in increased premixed combustion. This effect is emphasized in the blend mode compared to the DF mode because the injection of EtOH in the PFI mode reduces the local equivalence ratio in the diesel spray area and partially suppresses the premixed combustion stage. These results are supported by data presented in Figure 10. At 1500 rpm, the ID is −5° higher than the CDC for both EtOH modes. As the load and speed increase, the IDs are comparable, demonstrating that thermodynamic conditions in the combustion chamber have a more significant impact than the mixture characteristics. The blend mode has been observed to exert a more pronounced influence on the combustion process, although the tests were conducted at lower ethanol fractions than in the DF case. Indeed, the impact on CA10-50 is more pronounced, with a discrepancy of approximately 2° compared to DF for both operating points. Compared to the CDC case, there is a reduction of about 3°–4°, further confirming the hypothesis that predominant premixed combustion is more effective than the DF and CDC cases. About the CA50-90, it can be observed that at high load, the differences between the two modes diminish for the reasons previously outlined.

The blend combustion resulted in a higher peak of HRR compared to DF and CDC. This increased combustion noise, exceeding DF and CDC by −5 dBA (Figure 10) at 2000 rpm. This issue can be mitigated by appropriately optimizing the injection strategy for rail pressure, pilot quantity, and SOI [9, 61]. The COV_{IMEP} is acceptable and below 3% in all the combustion modes tested. At 7 bar of IMEP, the higher COV_{IMEP} value in DF mode relates to the high premixing nature of the mixture. At higher loads, the $_{IMEP}$ values are comparable.

The unburnt emissions of DF are one order of magnitude higher than the CDC and EtOH blend. The higher emissions of THC and CO may limit the EtOH fuel ratio in DF mode, particularly at low loads, because the ethanol cooling effect likely inhibits fuel atomization and vaporization, reducing combustion efficiency [62]. At 7 bar IMEP, the DF combustion significantly reduces smoke emissions (<0.2 FSN) compared to CDC (3.1 FSN). The EtOH blend decreases smoke emission to 0.5 FSN in this operating condition. At 10 bar IMEP, the DF smoke emissions exceed 1.3 FSN due to the high r_p and EGR combination that reduces the λ value. Indeed, despite the low carbon number of ethanol, the influence of λ is predominant in the DF case, resulting in an increased soot level. This demonstrates the limitations of DF combustion mode at higher loads and lower lambda values that may limit the maximum rated power output.

Figure 11 illustrates the energy distributions for both combustion modes, calculated according to the calculation scheme described in the methodology section in Figure 3. The main engine losses (incomplete combustion, exhaust, and in-cylinder HT) and η_{gross} are calculated. CDC generally emits lower CO and THC emissions, resulting in higher combustion efficiencies. The combustion losses calculated are below 0.5%. Blend combustion has combustion efficiencies like the CDC. Conversely, DF combustion results in higher combustion losses, up to −8% at 7 bar and −4.4% at 10 bar of IMEP. DF combustion exhibits lower η_{gross} by −6.2% (at 7 bar IMEP) and −1.2% (at 10 bar IMEP) than CDC. EtOH blend resulted in higher η_{gross} by −1.8% and −1.3% units compared to CDC for the lowest and highest loads tested, respectively. This is mainly due to reduced HT and exhaust enthalpy contents.

Table 5 reports the results of the Pugh matrix analysis based on seven engine performance criteria: THC + CO,

TABLE 5 Pugh matrix of ethanol combustion applications compared to CDC.

Criteria	CDC (datum)	Dual fuel	Blend
THC + CO		–	S
NOx		S	S
PM		+	+
CO_2		+	+
η_{gross}		–	+
COV_{IMEP}		–	S
Combustion noise		+	–
Total		**0**	**2**

NOx, PM, η_{gross}, COV_{IMEP}, and combustion noise. The comparison is referenced to the CDC performance. The symbols used are S in case of no difference, + in case of improvement, and – in case of deterioration. Summarizing, the ethanol blend is a valuable alternative to the CDC in terms of engine performance (emissions and efficiency), exhibiting a substantial PM reduction and efficiency improvement compared to DF and CDC. DF combustion resulted in lower PM emissions than CDC, but at the expense of lower efficiency and higher THC and CO emissions. Thus, based on the operating points investigated and the criteria within the scope of this study, the blend mode improves the emissions and efficiency behaviors than the other combustion modes studied. A possible approach for DF mode to address the increased THC and lower η_{gross} could be to properly design and optimize the combustion chamber (CR, bowl shape, reduced squish and crevice volumes) and the main engine calibration settings to reduce THC and enhance thermal efficiency.

Figure 12 reports a synthesis of the results available in the literature for ethanol-fueled engines, according to the two modes analyzed in the manuscript regarding PM, THC, and CO emissions. The data are based on CI engines of different sizes, speeds, and load conditions [16, 31, 53, 63–66]. The findings of the present study are consistent with the trends identified in the literature review. In particular, the blend mode demonstrates the advantage of lower PM and comparable THC and CO emissions compared to the CDC. Meanwhile, the DF mode shows

FIGURE 12 Experimental data collection based on the THC, CO, and PM emissions literature review for the investigated combustion modes (CDC, ethanol blend and DF).

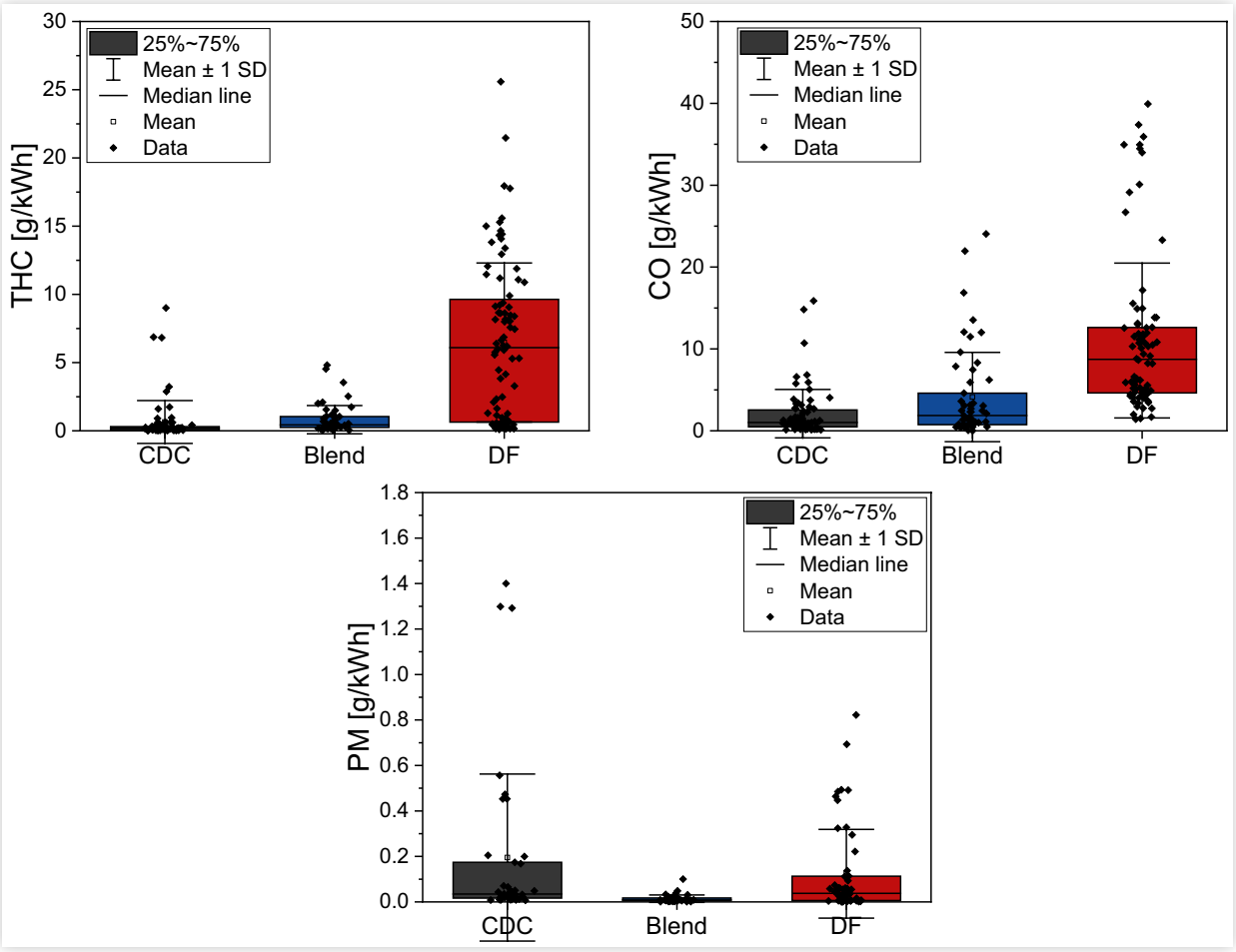

PM reduction but with consistently higher unburned emissions than the other combustion modes. Indeed, the blend mode proves to be the mode that most attenuates these differences with the CDC case. There is a substantial increase in the mean and standard deviation values for DF, while the blend mode assumes slightly higher values than the CDC.

4. Conclusions

Renewable ethanol as a low-carbon fuel is proposed as one of the possible strategies to reduce greenhouse gas emissions and local pollutant emissions. This study investigates the application of ethanol in a CI engine in DF and blend modes. The engine performance, combustion, and emission behaviors of EtOH combustion modes are compared to CDC. The main outcomes of this research are summarized below.

- DF and blend combustion exhibit significantly lower pilot HR than CDC. This is due to the high heat of vaporization of EtOH, which causes a longer ID, favoring a higher premixed combustion phase and shorter combustion duration. As the load and speed increase, the ID values are comparable, demonstrating that thermodynamic conditions in the combustion chamber have a greater impact than the mixture characteristics. Consequently, both fueling modes result in about a 2% improvement in indicated thermal efficiency and a 7.5% reduction in CO_2 compared to CDC at high NOx levels (8–12 g/kWh).
- Gross indicated efficiency (η_{gross}) for blend combustion is consistently higher than CDC (+1.8%) and DF mode (+8%) modes at ultra-low-NOx level (<1.0 g/kWh). This increase in η_{gross} is associated with a reduction in HT and exhaust losses and an enhancement in combustion efficiency. Additionally, a higher premixed combustion phase and shorter combustion duration with favorable CA50 further enhance η_{gross}.
- EtOH blend has similar combustion efficiency to CDC (–99.5%). It reduces significantly (–95%) in DF mode due to the high THC and CO emissions as a consequence of the fuel trapped in crevice and squish volumes partially or not involved in the combustion process. The THC and CO emissions of EtOH blend are comparable to the CDC.
- Ethanol-based fuels are known to promote low-soot combustion across a broad range of equivalence ratios, resulting in a relatively flat NO_x–soot trade-off compared to CDC. Ethanol, when used in DF configurations or blended with diesel, very low smoke emissions (–0.1 FSN) largely independent of the associated NO_x levels. This favorable behavior is attributed to ethanol's molecular structure, which consists of a short carbon chain and an OH functional group. The low carbon-to-hydrogen ratio and oxygenated nature of EtOH hinder the formation of PAH precursors, which are critical intermediates in soot formation.
- In both DF and blend modes, the COV_{IMEP} is in line with CDC. This indicates that even in DF mode with a higher EtOH fraction (70%), small amounts of high-reactive fuels help to stabilize the combustion process. The peak pressure rise rate affects the combustion noise. The combustion noise is consistently higher (5 dBA) for the blend mode compared to DF and CDC values. This drawback can be addressed by properly calibrating the injection pattern, EGR, and boosting parameters.

Alternative fuels, such as ethanol, can be applied in different fueling and combustion modes and can potentially balance NOx and CO_2 emissions without degradation of soot emissions within the NOx range explored. For a real application, DF needs significant modifications to the engine, two fuel tanks, an additional fuel injection system, and a control system. A dedicated combustion chamber, calibration refinement, and specific ATS are required to mitigate the THC and CO emissions. On the other hand, blending EtOH with diesel up to a certain level (30% EtOH with biodiesel as solubilizer) enables the application on standard production engines with potential benefits on CO_2 emissions, lower soot and CO and THC emissions like CDC.

Acknowledgements

The authors acknowledge Alessio Schiavone and Augusto Piccolo for their technical support in making the test cell operative for the experimental test execution.

Declaration of Competing Interest

The authors declare that they have no known competing financial interests or personal relationships that could have appeared to influence the work reported in this article.

The authors and SAE International declare that two of the authors of this article are on the editorial board of the journal. SAE warrants that confidentiality was maintained throughout the peer-review process and no partiality was granted to the work. SAE further warrants that the editorial board members had no influence and did not take part in any type of decision making or peer review.

Contact Information

Gabriele Di Blasio
gabriele.diblasio@cnr.it

Giacomo Belgiorno
giacomo.belgiorno@dumarey.com

Roberto Ianniello
roberto.ianniello@stems.cnr.it

Highlights

- Ethanol–diesel dual-fuel combustion emits higher levels of THC and CO compared to the blend mode.
- Ethanol facilitates low-soot combustion, particularly in ultra-low-NOx emission zones.
- Ethanol blend combustion achieves greater thermal efficiency and noise but lower COV_{IMEP} than CDC.
- A novel comparative study is conducted on dual-fuel and blend combustion modes using a single test rig.

Abbreviations

aTDC - After top-dead center
bTDC - Before top-dead center
CA10 - deg where 10% of total heat releases
CA50 - deg where 50% of total heat releases
CA90 - deg where 90% of total heat releases
CA10-90 - Combustion duration
CAD - Crank angle degree
CDC - Conventional diesel combustion
CI - Compression ignition
CN - Cetane number
COV_{IMEP} - Coefficient of variation of IMEP
DF - Dual fuel
EGR - Exhaust gas recirculation
EtOH - Ethanol
HRR - Apparent heat release rate
HT - Heat transfer
ID - Ignition delay
IMEP - Indicated mean effective pressure
LHV - Lower heating value
NEDC - New European drive cycle
NOx - Nitrogen oxides
RON - Research octane number
PAH - Polycyclic aromatic hydrocarbon
PFI - Port fuel injection
PPC - Partially premixed combustion
SCE - Single-cylinder engine
SI - Spark ignition
SOI - Start of injection
TDC - Top-dead center
WLTC - Worldwide Harmonized Light Vehicle Test Cycles
$\dot{W}_{gross}$ - Gross indicated work
λ - Equivalence air–fuel ratio
η_{comb} - Combustion efficiency
η_{gross} - Gross indicated efficiency

References

1. Joshi, A., "Year in Review: Progress towards Decarbonizing Transport and Near-Zero Emissions," SAE Technical Paper 2023-01-0396 (2023), doi:https://doi.org/10.4271/2023-01-0396.
2. IEA – International Energy Agency, "Global Energy and Climate Model," accessed October 15, 2024, https://www.iea.org/reports/global-energy-and-climate-model.
3. Ritchie, H. and Roser, M., "Sector by Sector: Where Do Global Greenhouse Gas Emissions Come From?" Our World in Data, 2024, accessed October 15, 2024, https://ourworldindata.org/ghg-emissions-by-sector.
4. Chiaramonti, D., Talluri, G., Scarlat, N., and Prussi, M., "The Challenge of Forecasting the Role of Biofuel in EU Transport Decarbonisation at 2050: A Meta-Analysis Review of Published Scenarios," *Renewable and Sustainable Energy Reviews* 139 (2021): 110715, doi:https://doi.org/10.1016/j.rser.2021.110715.
5. Mousdale, D.M., "Past, Present and Future: A Role for Liquid Biofuels in Transitioning to Net Zero?" *Natural Resources* 15 (2024): 107-124, doi:https://doi.org/10.4236/nr.2024.155008.
6. Agarwal, A.K., "Biofuels (Alcohols and Biodiesel) Applications as Fuels for Internal Combustion Engines," *Progress in Energy and Combustion Science* 33 (2007): 233-271, doi:https://doi.org/10.1016/j.pecs.2006.08.003.
7. Verhelst, S., Turner, J.W., Sileghem, L., and Vancoillie, J., "Methanol as a Fuel for Internal Combustion Engines," *Progress in Energy and Combustion Science* 70 (2019): 43-88, doi:https://doi.org/10.1016/j.pecs.2018.10.001.
8. Pedrozo, V.B., May, I., Guan, W., and Zhao, H., "High Efficiency Ethanol-Diesel Dual-Fuel Combustion: A Comparison against Conventional Diesel Combustion from Low to Full Engine Load," *Fuel* 230 (2018): 440-451, doi:https://doi.org/10.1016/j.fuel.2018.05.034.
9. Belgiorno, G., Dimitrakopoulos, N., Di Blasio, G., Beatrice, C. et al., "Effect of the Engine Calibration Parameters on

Gasoline Partially Premixed Combustion Performance and Emissions Compared to Conventional Diesel Combustion in a Light-Duty Euro 6 Engine," *Applied Energy* 228 (2018): 2221-2234, doi:https://doi.org/10.1016/j.apenergy.2018.07.098.

10. Kaliyan, N., Morey, R.V., and Tiffany, D.G., "Reducing Life Cycle Greenhouse Gas Emissions of Corn Ethanol by Integrating Biomass to Produce Heat and Power at Ethanol Plants," *Biomass and Bioenergy* 35 (2011): 1103-1113, doi:https://doi.org/10.1016/j.biombioe.2010.11.035.
11. Kheshgi, H.S. and Prince, R.C., "Sequestration of Fermentation CO_2 from Ethanol Production," *Energy* 30 (2005): 1865-1871, doi:https://doi.org/10.1016/j.energy.2004.11.004.
12. Gautam, M. and Martin, D.W., "Combustion Characteristics of Higher-Alcohol/Gasoline Blends," *Proceedings of the Institution of Mechanical Engineers, Part A: Journal of Power and Energy* 214 (2000): 497-511, doi:https://doi.org/10.1243/0957650001538047.
13. Sahu, T.K., Shukla, P.C., Belgiorno, G., and Maurya, R.K., "Alcohols as Alternative Fuels in Compression Ignition Engines for Sustainable Transportation: A Review," *Energy Sources, Part A: Recovery, Utilization, and Environmental Effects* 44 (2022): 8736-8759, doi:https://doi.org/10.1080/15567036.2022.2124326.
14. Shen, M., Tuner, M., Johansson, B., Shen, M. et al., "Close to Stoichiometric Partially Premixed Combustion -The Benefit of Ethanol in Comparison to Conventional Fuels," SAE Technical Paper 2013-01-0277 (2013), doi:https://doi.org/10.4271/2013-01-0277.
15. Kaiadi, M., Johansson, B., Lundgren, M., and Gaynor, J.A., "Sensitivity Analysis Study on Ethanol Partially Premixed Combustion," *SAE Int. J. Engines* 6, no. 1 (2013): 120-131, doi:https://doi.org/10.4271/2013-01-0269.
16. Shamun, S., Belgiorno, G., Di Blasio, G., Beatrice, C. et al., "Performance and Emissions of Diesel-Biodiesel-Ethanol Blends in a Light Duty Compression Ignition Engine," *Applied Thermal Engineering* 145 (2018): 444-452, doi:https://doi.org/10.1016/j.applthermaleng.2018.09.067.
17. Shahir, S.A., Masjuki, H.H., Kalam, M.A., Imran, A. et al., "Feasibility of Diesel–Biodiesel–Ethanol/Bioethanol Blend as Existing CI Engine Fuel: An Assessment of Properties, Material Compatibility, Safety and Combustion," *Renewable and Sustainable Energy Reviews* 32 (2014): 379-395, doi:https://doi.org/10.1016/j.rser.2014.01.029.
18. Pradelle, F., Braga, S.L., de Aguiar Martins, A.R.F., Turkovics, F. et al., "Stabilization of Diesel–Biodiesel–Ethanol (DBE) Blends: Formulation of an Additive from Renewable Sources," *J Braz. Soc. Mech. Sci. Eng.* 39 (2017): 3277-3293, doi:https://doi.org/10.1007/s40430-017-0862-1.
19. Agarwal, A., Singh, A., Kumar, V., Sharma, N. et al., "Alcohol-Fueled Reactivity-Controlled Compression Ignition Combustion for Partial Replacement of Mineral Diesel in Internal Combustion Engines," *SAE Int. J. Engines* 14, no. 6 (2021): 785-804, doi:https://doi.org/10.4271/03-14-06-0047.
20. Garg, R., Mukherjee, N., Viswanath, C., Choudhary, V. et al., "Effect of Diesel-Ethanol Blends on the Performance and Emissions of a CI Diesel Engine Suitable for Stationary Application," SAE Technical Paper 2024-26-0078 (2024), doi:https://doi.org/10.4271/2024-26-0078.
21. Fayad, M.A., Tsolakis, A., and Martos, F.J., "Influence of Alternative Fuels on Combustion and Characteristics of Particulate Matter Morphology in a Compression Ignition Diesel Engine," *Renewable Energy* 149 (2020): 962-969, doi:https://doi.org/10.1016/j.renene.2019.10.079.
22. Belgiorno, G., Di Blasio, G., Shamun, S., Beatrice, C. et al., "Performance and Emissions of Diesel-Gasoline-Ethanol Blends in a Light Duty Compression Ignition Engine," *Fuel* 217 (2018): 78-90, doi:https://doi.org/10.1016/j.fuel.2017.12.090.
23. Pidol, L., Lecointe, B., Starck, L., and Jeuland, N., "Ethanol–Biodiesel–Diesel Fuel Blends: Performances and Emissions in Conventional Diesel and Advanced Low Temperature Combustions," *Fuel* 93 (2012): 329-338, doi:https://doi.org/10.1016/j.fuel.2011.09.008.
24. Satgé de Caro, P., Mouloungui, Z., Vaitilingom, G., and Berge, J.C., "Interest of Combining an Additive with Diesel–Ethanol Blends for Use in Diesel Engines," *Fuel* 80 (2001): 565-574, doi:https://doi.org/10.1016/S0016-2361(00)00117-4.
25. Padala, S., Woo, C., Kook, S., and Hawkes, E.R., "Ethanol Utilisation in a Diesel Engine Using Dual-Fuelling Technology," *Fuel* 109 (2013): 597-607, doi:https://doi.org/10.1016/j.fuel.2013.03.049.
26. Asad, U., Zheng, M., and Tjong, J., "Experimental Investigation of Diesel-Ethanol Premixed Pilot-Assisted Combustion (PPAC) in a High Compression Ratio Engine," *SAE Int. J. Engines* 9, no. 2 (2016): 1059-1071, doi:https://doi.org/10.4271/2016-01-0781.
27. Beatrice, C., Denbratt, I., Di Blasio, G., Di Luca, G. et al., "Experimental Assessment on Exploiting Low Carbon Ethanol Fuel in a Light-Duty Dual-Fuel Compression Ignition Engine," *Applied Sciences* 10 (2020): 7182, doi:https://doi.org/10.3390/app10207182.
28. Gawale, G.R. and Naga Srinivasulu, G., "Experimental Investigation of Ethanol/Diesel and Ethanol/Biodiesel on Dual Fuel Mode HCCI Engine for Different Engine Load Conditions," *Fuel* 263 (2020): 116725, doi:https://doi.org/10.1016/j.fuel.2019.116725.
29. Gargiulo, V., Alfè, M., Di Blasio, G., and Beatrice, C., "Chemico-Physical Features of Soot Emitted from a Dual-Fuel Ethanol–Diesel System," *Fuel* 150 (2015): 154-161, doi:https://doi.org/10.1016/j.fuel.2015.01.096.
30. Heywood, J.B., *Internal Combustion Engine Fundamentals*, 2nd ed. (New York: McGraw-Hill Education, 2018). https://www.accessengineeringlibrary.com/content/book/9781260116106
31. Heuser, B., Kremer, F., Pischinger, S., Rohs, H. et al., "An Experimental Investigation of Dual-Fuel Combustion in a Light Duty Diesel Engine by In-Cylinder Blending of

Ethanol and Diesel," *SAE Int. J. Engines* 9, no. 1 (2015): 11-25, doi:https://doi.org/10.4271/2015-01-1801.

32. Torres-Jimenez, E., Jerman, M.S., Gregorc, A., Lisec, I. et al., "Physical and Chemical Properties of Ethanol–Diesel Fuel Blends," *Fuel* 90 (2011): 795-802, doi:https://doi.org/10.1016/j.fuel.2010.09.045.
33. Stein, R.A., Anderson, J.E., Wallington, T.J., Stein, R.A. et al., "An Overview of the Effects of Ethanol-Gasoline Blends on SI Engine Performance, Fuel Efficiency, and Emissions," *SAE Int. J. Engines* 6, no. 1 (2013): 470-487, doi:https://doi.org/10.4271/2013-01-1635.
34. Ra, Y., Reitz, R.D., McFarlane, J., Daw, C.S. et al., "Effects of Fuel Physical Properties on Diesel Engine Combustion using Diesel and Bio-Diesel Fuels," *SAE Int. J. Fuels Lubr.* 1, no. 1 (2009): 703-718, doi:https://doi.org/10.4271/2008-01-1379.
35. Woods, J., *Sustainable Biofuels: Prospects and Challenges* (London: The Royal Society, 2008)
36. Pecchia, M.D., Pessina, V., Iacovano, C., and Cantore, G., "Development of Gasoline-Ethanol Blends Laminar Flame Speed Correlations at Full-Load SI Engine Conditions via 1D Simulations," *AIP Conference Proceedings* 2191 (2019): 020063, doi:https://doi.org/10.1063/1.5138796.
37. Lapuerta, M., Garcia-Contreras, R., and Agudelo, J.R., "Lubricity of Ethanol-Biodiesel-Diesel Fuel Blends," *Energy & Fuels* 24 (2010): 1374-1379.
38. EUR-Lex, "Directive—2009/30—EN," accessed October 15, 2024, https://eur-lex.europa.eu/eli/dir/2009/30/oj.
39. Chakradhar, M., Chakrahari, K.K., Prakash, S., Raj, J. et al., "Development of Oxygenated Diesel Fuel and Impact on Vehicle Performance," SAE Technical Paper 2024-01-2374 (2024), doi:https://doi.org/10.4271/2024-01-2374.
40. Barabás, I. and Todorut, I.-A., "Predicting the Temperature Dependent Viscosity of Biodiesel–Diesel–Bioethanol Blends," *Energy & Fuels* 25 (2011): 5767-5774.
41. Barabás, I., Todoruţ, A.I., Barabás, I., and Todoruţ, A.I., "Key Fuel Properties of Biodiesel-Diesel Fuel-Ethanol Blends," SAE Technical Paper 2009-01-1810 (2009), doi:https://doi.org/10.4271/2009-01-1810.
42. Barabas, I., Todoruţ, A., and Cordoş, N., "An Artificial Neural Network Approach to Estimate the Viscosity of Biodiesel-Diesel-Ethanol Blends," *Acta Technica Napocensis-Series: Applied Mathematics, Mechanics, and Engineering* 59, no. 3 (2016): 157-162.
43. Krzemiński, A. and Ustrzycki, A., "Effect of Ethanol Added to Diesel Fuel on the Range of Fuel Spray," *Energies* 16 (2023): 1768.
44. Kuszewski, H., Jaworski, A., and Mądziel, M., "Lubricity of Ethanol–Diesel Fuel Blends—Study with the Four-Ball Machine Method," *Materials* 14 (2021): 2492, doi:https://doi.org/10.3390/ma14102492.
45. Low, M., Mukhtar, N., Hagos, F.Y., and Noor, M., "Tri-Fuel (Diesel-Biodiesel-Ethanol) Emulsion Characterization, Stability and the Corrosion Effect," *IOP Conference Series: Materials Science and Engineering* 257 (2017): 012082.
46. Joumaa, C., Saad, I., and Younes, G., "Effect of Diesel-Biodiesel-Ethanol Mixtures on Corrosion Rate of Various Metals in the Presence of Tert-Butylhydroquinone (TBHQ)," *Química Nova* 47 (2024): e-20230083.
47. Soares, M., Berbel, L.O., Vieira, C., Oliszeski, D. et al., "Study of Corrosion of AA 3003 Aluminum in Biodiesel, Diesel, Ethanol and Gasoline Media," *Materials Science Forum* 1012 (2020): 407-411.
48. Ianniello, R., Belgiorno, G., Di Luca, G., Beatrice, C. et al., "Ethanol in Dual-Fuel and Blend Fueling Modes for Advanced Combustion in Compression Ignition Engines," in: Shukla, P.C., Belgiorno, G., Di Blasio, G., Agarwal, A.K. (eds.), *Alcohol as an Alternative Fuel for Internal Combustion Engines* (Singapore: Springer, 2021), 5-27, https://doi.org/10.1007/978-981-16-0931-2_2.
49. Belgiorno, G., Di Blasio, G., and Beatrice, C., "Parametric Study and Optimization of the Main Engine Calibration Parameters and Compression Ratio of a Methane-Diesel Dual Fuel Engine," *Fuel* 222 (2018): 821-840, doi:https://doi.org/10.1016/j.fuel.2018.02.038.
50. Fraioli, V., Beatrice, C., Blasio, G.D., Belgiorno, G. et al., "Multidimensional Simulations of Combustion in Methane-Diesel Dual-Fuel Light-Duty Engines," SAE Technical Paper 2017-01-0568 (2017), doi:https://doi.org/10.4271/2017-01-0568.
51. Blasio, G.D., Beatrice, C., Molina, S., Blasio, G.D. et al., "Effect of Port Injected Ethanol on Combustion Characteristics in a Dual-Fuel Light Duty Diesel Engine," SAE Technical Paper 2013-01-1692 (2013), doi:https://doi.org/10.4271/2013-01-1692.
52. Kim, K.H., Choi, B., Park, S., Kim, E. et al., "Emission Characteristics of Compression Ignition (CI) Engine Using Diesel Blended with Hydrated Butanol," *Fuel* 257 (2019): 116037, doi:https://doi.org/10.1016/j.fuel.2019.116037.
53. Kumar, V., Singh, A.P., and Agarwal, A.K., "Gaseous Emissions (Regulated and Unregulated) and Particulate Characteristics of a Medium-Duty CRDI Transportation Diesel Engine Fueled with Diesel-Alcohol Blends," *Fuel* 278 (2020): 118269, doi:https://doi.org/10.1016/j.fuel.2020.118269.
54. Thongchai, S., Lim, O., and Tongroon, M., "The Effect of Injection Strategy and Ternary Ethanol Blend on the Spray Behavior and Its Resultant on Combustion Characteristics," *Renewable Energy* 243 (2023): 122479, doi:https://doi.org/10.2139/ssrn.4624811.
55. Idicheria, C.A., Pickett, L.M., Idicheria, C.A., and Pickett, L.M., "Soot Formation in Diesel Combustion under High-EGR Conditions," SAE Technical Paper 2005-01-3834 (2005), doi:https://doi.org/10.4271/2005-01-3834.
56. Sahu, T.K., Shukla, P.C., Mondal, A., Gupta, S. et al., "Assessment of Particulate PAHs Toxicity from Alcohol-Diesel Blends Fuelled High Compression Ratio CI Engine," *Cleaner Engineering and Technology* 18 (2024): 100725, doi:https://doi.org/10.1016/j.clet.2024.100725.

57. Maricq, M.M., "Chemical Characterization of Particulate Emissions from Diesel Engines: A Review," *Journal of Aerosol Science* 38 (2007): 1079-1118.
58. Shamun, S., Novakovic, M., Malmborg, V.B., Preger, C. et al., "Detailed Characterization of Particulate Matter in Alcohol Exhaust Emissions," in *9th International Conference on Modeling and Diagnostics for Advanced Engine Systems, COMODIA 2017*, Okayama, Japan, 2017, B304, The Japan Society of Mechanical Engineers.
59. Sarjovaara, T. and Larmi, M., "Dual Fuel Diesel Combustion with an E85 Ethanol/Gasoline Blend," *Fuel* 139 (2015): 704-714, doi:https://doi.org/10.1016/j.fuel.2014.09.049.
60. Lee, S., Kim, C., Lee, S., Oh, S. et al., "Characteristics of Non-Methane Hydrocarbons and Methane Emissions in Exhaust Gases under Natural-Gas/Diesel Dual-Fuel Combustion," *Fuel* 290 (2021): 120009, doi:https://doi.org/10.1016/j.fuel.2020.120009.
61. Belgiorno, G., Dimitrakopoulos, N., Blasio, G.D., Beatrice, C. et al., "Parametric Analysis of the Effect of Pilot Quantity, Combustion Phasing and EGR on Efficiencies of a Gasoline PPC Light-Duty Engine," SAE Technical Paper 2017-24-0084 (2017), doi:https://doi.org/10.4271/2017-24-0084.
62. Wu, Y., Zhang, X., Zhang, Z., Wang, X. et al., "Effects of Diesel-Ethanol-THF Blend Fuel on the Performance and Exhaust Emissions on a Heavy-Duty Diesel Engine," *Fuel* 271 (2020): 117633, doi:https://doi.org/10.1016/j.fuel.2020.117633.
63. Damyanov, A. and Hofmann, P., "Operation of a Diesel Engine with Intake Manifold Alcohol Injection," in: Springer Nature, *Internationaler Motorenkongress 2019* (Wiesbaden, Germany: Springer, 2019), 313-332.
64. Ning, L., Duan, Q., Chen, Z., Kou, H. et al., "A Comparative Study on the Combustion and Emissions of a Non-Road Common Rail Diesel Engine Fueled with Primary Alcohol Fuels (Methanol, Ethanol, and n-Butanol)/Diesel Dual Fuel," *Fuel* 266 (2020): 117034, doi:https://doi.org/10.1016/j.fuel.2020.117034.
65. Chen, Z., Wang, L., and Zeng, K., "A Comparative Study on the Combustion and Emissions of Dual-Fuel Engine Fueled with Natural Gas/Methanol, Natural Gas/Ethanol, and Natural Gas/n-Butanol," *Energy Conversion and Management* 192 (2019): 11-19.
66. Saccullo, M., Nygren, A., Benham, T., and Denbratt, I., "Alcohol Flexible HD Single Cylinder Diesel Engine Tests with Separate Dual High Pressure Direct Fuel Injection," *Fuel* 294 (2021): 120478, doi:https://doi.org/10.1016/j.fuel.2021.120478.